Available online at www.sciencedirect.com
SCIENCE DIRECT®
Polymer 45 (2004) 3885–3891
polymer
www.elsevier.com/locate/polymer

Molecular dynamics studies on the effects of water speciation on interfacial structure and dynamics in silica-filled PDMS composites☆

Richard H. Gee*, Robert S. Maxwell, Bryan Balazs

Lawrence Livermore National Laboratory, Chemistry and Material Science Directorate, University of California, Livermore, CA 94550, USA

Received 17 May 2003; received in revised form 7 January 2004; accepted 7 January 2004

Abstract

The effect of chemisorbed and physisorbed water on the interfacial structure and dynamics in silica-filled polydimethylsiloxane (PDMS) based composites have been investigated. Toward this end, we have combined molecular dynamics simulations and experimental studies employing dynamic mechanical analysis and nuclear magnetic resonance analysis. Our results suggest that the polymer–silica contact distance and the mobility of interfacial polymer chains significantly decreased as the hydration level at the interface was reduced. The reduced mobility of the PDMS chains in the interfacial domain reduced the overall, bulk, motional properties of the polymer, thus causing an effective 'stiffening' of the polymer matrix. The role of the long-ranged Coulombic interactions on the structural features and chain dynamics of the polymer were also examined. Both are found to be strongly influenced by the electrostatic interactions as identified by the bond orientation time correlation function, local density distribution and radial distribution functions. These results have important implications for the design and life performance behavior of nanocomposite silica–siloxane materials.

Keywords: Polydimethylsiloxane; Molecular dynamics; Interfacial dynamics

1. Introduction

Silica-filled polydimethylsiloxane (PDMS) composite systems are of broad appeal due to their chemical and environmental resilience and the availability of a wide range of tailorable chemical and mechanical properties [1–3]. This versatility is due, at least in part, to the presence of inorganic filler materials which are well know to significantly alter polymer material mechanical properties [4]. Understanding of the interfacial chemistry is important for the ultimate engineering of mechanical, electrical, or chemical properties. The reinforcing mechanisms that control the material property changes in polymer–silica composite materials, for example, are poorly understood and rational control of the mechanical properties is difficult and often based solely on empirical correlations [4]. With the large financial investment by the polymer industry in filled polymers and the increased interest in organic-inorganic nanocomposite materials, in-depth studies of interfacial interactions between filler surfaces and associated polymer chains are warranted.

In this paper, we use molecular dynamics (MD) and to study the effects of fillers on a PDMS polymer at the molecular level, which provides an ideal opportunity for direct insight into the interfacial structure and dynamics.

The primary reinforcing mechanism by which silica fillers are thought to alter the properties of siloxane-based polymeric materials is via hydrogen bonding interactions [4]. In an effort to gain further insight into the reinforcing mechanisms of inorganic fillers on PDMS based composites, we have initiated a computational study of the effects of changes in interfacial hydroxyl content on the chain dynamics of adsorbed PDMS chains. The data obtained in this study have implications on rational engineering of PDMS–silica materials, chemical aging of composite materials, and future design of nano-scale inorganic–organic composite materials.

The computational results presented here of segmental dynamics at various hydration levels predict that removal of water from the silica surface should cause a reduction in the segmental dynamics of the adsorbed polymer chains. These

☆ Supplementary data associated with this article can be found on the online version of this article

* Corresponding author. Tel.: +1-925-423-1177.
E-mail address: gee10@llnl.gov (R.H. Gee).

0032-3861/$ - see front matter © 2004 Elsevier Ltd. All rights reserved.
doi:10.1016/j.polymer.2004.01.078

results are compared to experimental results studying thermal behavior as studied by differential scanning calorimetry (DSC), and segmental dynamics, as studied by nuclear magnetic resonance (NMR), as a function of time stored in a desiccating environment. The experimental and computational results obtained in this study show that silica-filled PDMS/PDPS copolymers undergo time dependent hardening in desiccating environments.

2. Computational methods

2.1. Polymer-filler representation

The MD simulations of silica/PDMS composites were carried out using three dimensional periodic arrays of orthorhombic unit cells containing one unbranched PDMS polymer chain of 120 dimethylsiloxane monomer units. The use of single chain polymers to represent amorphous melts and glasses is common, and has proven to be quite accurate in replicating the behavior of experimental polymeric systems [5–16]. The PDMS chains were then introduce onto a silica surface with the approximate dimensions of 22×22 Å, and a thickness of ~ 15 Å. The actual cell length normal to the silica surface was chosen such that the PDMS interfaced to the silica surface did not interact with its periodic image. The PDMS melt, therefore, experiences both a solid and vacuum interface. The number of surface hydroxyl groups found on the silica surface was also varied so as to allow for the direct elucidation of the effects of hydrogen bonding interactions between the polymer and filler surface. The hydroxyl content ranged between that of a dehydrated silica surface (zero hydroxyl groups) to one with twice the average number of groups per unit area, as determined experimentally [17] (i.e., ≈ 8OH/100 Å^2). Simulations were also performed with a layer of physisorbed water placed at the PDMS/silica interface, where the physisorbed water molecules were randomly placed and free to move and dynamically adjust throughout the simulations. All atoms in the system were treated explicitly.

The initial polymer starting configurations were generated using a Monte Carlo method [18]. The monomers were allowed to 'polymerize' in a head-to-tail manner with no monomer reversals. The resulting amorphous structure along with the silica surface was then relaxed by energy minimization.

2.2. Potential functions

The MD simulations of the polymer silica composite employ the CFF91 [19–21] force field parameter set. The CFF91 potential consists of valence terms including diagonal and off diagonal cross coupling terms, and non-bonded van der Waals and Coulombic interaction terms. The functional form of the potential employs a quartic polynomial for bond stretching and angle bending and a three-term Fourier expansion for torsions. The out-of-plane coordinate was defined according to Wilson et al. [22]. The atomic charges for the non-bonded Coulombic interaction are derived from ab initio calculations. The van der Waals interactions were implemented using a Lennard–Jones (LJ) potential, making use of an inverse 9th-power term for the repulsive part rather than the more customary 12th-power term. The CFF91 non-bonded potential accounts for the hydrogen bonding implicitly through the parameterization of the ab initio based force field [19–21].

All valence degrees of freedom were explicitly treated and unconstrained. The Coulombic interactions were calculated by employing the standard Ewald method [23,24], while the van der Waals interactions were truncated for atom pairs with an inter-atomic distance greater than 11 Å.

2.3. Molecular dynamics method

The polymer silica composite simulations were performed using constant particle number, volume, and temperature (*NVT*) dynamics. The Verlet velocity [25] time integration method was used with a time step of 0.5 fs. The Andersen [26] method was used for constant particle, volume and temperature (NVT) dynamics. All structures were initially simulated at 550 K for a minimum duration of 1 ns so as to equilibrate the system, followed by a data collection period of a minimum of the same.

All computations were carried out with the DISCOVER commercial software program from Molecular Simulations, Inc. [18].

3. Experimental methods

Experimental studies were performed on a composite materials designed to meet specific service requirements by LLNL, including extended service life. The materials were a crosslinked copolymer of 90.7 wt% PDMS and 9.0 wt% PDPS. The copolymer gum was filled with 21.6 wt% Cab-o-Sil M7D silica (NuSil Corp., Carpenteria, CA) and 4 wt% Hi-sil 233 precipitated silica (PPG Industries Inc., Pittsburg, PA) fillers previously reacted with 6.8 wt% ethoxy-end-blocked PDMS processing aid (Y1587, Union Carbide Corp. Danbury, CT) [27,28].

For DSC analysis, samples were subject to an 8 h, 70 °C bake out and subsequent storage in a nitrogen-purged, desiccated box for 6 months. The samples were then placed in hermetically sealed DSC pans, which were coated with Parylene™ to further protect against moisture ingress. Analysis was performed with a TA instruments Model Q1000 DSC under a 50 ml/min He purge and a 3 °C/min ramp rate. DSC analysis of hydrated samples with and without the Parylene™ coating were indistinguishable, suggesting that the contribution to the DSC results was negligible. A container with 'Drierite™' was used for storage except when the samples were being analyzed.

Polymer chain dynamics were measured using a ^{1}H NMR spin-echo approach that has been described previously [27,28]. In PDMS-based polymers the dipolar coupling between neighboring protons is reduced due to anisotropic fast motional processes to ~1% of the static value. This residual dipolar coupling is sensitive to changes in the average chain length and thus crosslink density. For the case of Gaussian chain statistics, the observed mean residual dipolar coupling is predicted to be proportional to the crosslink density [29,30]:

$$\langle \Omega_d^2 \rangle = AN^{-2} = A\upsilon_{total}^2. \quad (1)$$

Dipolar couplings in solids can be measured by their effects on spin-spin relaxation times via second moment analysis [31], double quantum methods [32–35], or echo decay methods [29,36]. In cases where the correlation time for the residual dipolar couplings remains fairly unchanged, the decay of transverse magnetization in a spin-echo experiment simplifies to

$$E(t) = \exp(-t/T_2 - t^2\langle \Omega_d^2 \rangle). \quad (2)$$

A further simplification can be made in cases where the second term in the exponential is dominant but small enough that the decay is still fairly exponential, i.e. the curvature of the decay in minimal:

$$E(t) = \exp(-\langle \Omega_d^2 \rangle t) = \exp(-t1/T_{2e}). \quad (3)$$

where $1/T_{2e}$ is the effective transverse relaxation time and is proportional to $\langle \Omega_d^2 \rangle$,

$$1/T_{2e} \propto \langle \Omega_d^2 \rangle \propto \nu_{total}^2. \quad (4)$$

Further, from rubber elasticity theory:

$$G' = pRT/MW_{cl} = pRT\upsilon_{total}. \quad (5)$$

Thus, $1/T_{2e} \propto G'^2$ and can serve as a convenient indirect measure of changes in mechanical properties in controlled atmospheres where direct measure is inconvenient or impossible.

For NMR analysis, a small sample of polymer was sealed in a 5 mm NMR tube with a small amount of desiccant positioned so that only the polymer was within the receiver coil volume; this sample was then aged for up to 1 year and transverse relaxation times were measured periodically by spin-echo methods [27,28,37]. Seven microseconds π/2 pulse lengths, 7-second relaxation delays, and a standard Bruker 5 mm TBI probe were used on a Bruker DRX-500 NMR spectrometer [Bruker Biospin, Bilerica, MA]. The echo decay curves were analyzed by measuring the time to reach $1/e$ of the initial intensity, T_{2e}, after removing the effects of the contribution to the decay of the sol fraction of the polymer (~10% of the echo decay curve).

Dynamic mechanical analysis (DMA) testing was performed (TA Instruments AR2000 Rheometer, New Castle, Delaware) in parallel plate geometry. Specimens were disks approximately 2 mm in thickness and 8 mm in diameter. The sample was sheared at a frequency of $f = 6.3$ rad/s. For room temperature shear storage modulus measurements, samples were sheared up to 1% strain level with a static compression force of 1 N.

4. Results and discussion

4.1. Experimental

DSC thermograms for the virgin filled polymer and the filled polymer aged for 6 months over Drierite™ are shown in Fig. 1. For both samples, T_g was observed at −117 °C, while for desiccated samples, T_g was accompanied by a simultaneous stress relaxation of 0.75 J/g in the non-reversible heat flow measurement. In addition, a double melt peak was observed for both samples. Double melt peaks have been observed previously in PDMS polymer systems and are thought to be melting events in similar, but distinct structural phases. The dual melting peaks are proposed to be the result of partial crystallization that occurs during both the cooling and heating cycles due to ramp rate effects. The first melt peak was invariant with desiccation ($T_{m1} = -78.5$ °C) while the second melt peak shifted slightly to a lower temperature upon desiccation ($\Delta T_{m2} = -3.3$ °C). The heat of fusion also decreased slightly upon desiccation ($\Delta H_f = 9.4$ J/g hydrated and $\Delta H_f = 8.8$ J/g desiccated). Further, the melt feature as a whole shifted from predominantly reversible heat flow for hydrated samples to predominantly non-reversible heat flow for desiccated samples. A small amount of recrystallization heat flow was observed for hydrated samples immediately following the second melt peak. This feature was absent in the desiccated sample. After 24 h, the DSC pan for the desiccated sample was punctured, exposed to air, and rerun. The DSC thermogram was consistent with a fully hydrated sample, suggesting that the changes observed upon desiccation were reversible, thus due to the action of the

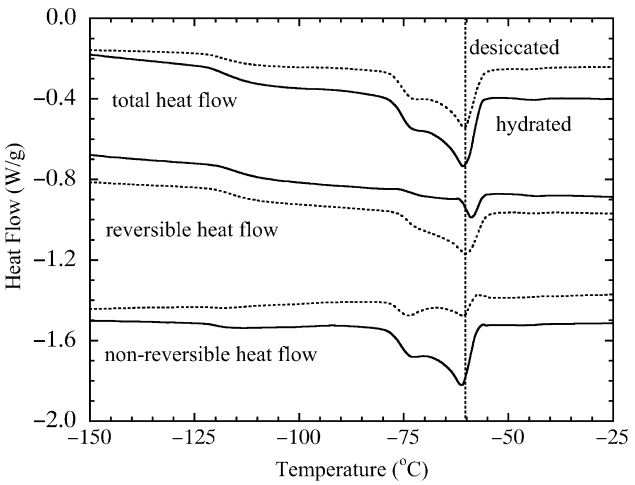

Fig. 1. DSC thermograms of the copolymer at ambient conditions (solid curve), and the copolymer after 6 months desiccation (dotted curve).

desiccant rather than an irreversible chemical reaction. The origin of these observations is unknown based on the DSC studies alone, thus, a modeling studies may help provide a molecular level understanding of the changes (see Section 4.2).

The results of the spin-echo relaxation time experiments on desiccated samples are shown in Fig. 2. For this system, we have verified that the NMR relaxation times reflect changes in polymer mechanical properties by comparing relaxation times and storage modulus for a series of materials with variable crosslink density. The results of this study are shown in Fig. 3. The desiccation NMR experiments show that as the polymer material was aged in the presence of desiccating agents with various relative affinities for water, the polymer segmental dynamics were seen to slow down over the course of one year. Based on the correlation established in Fig. 3, this change corresponds to a change in G' after 1 year of $\sim$30%. Additionally, the relative stiffening ability of the various desiccating agents was observed to be roughly consistent with their affinities for water (LiH > P_2O_5 > mol sieves).

4.2. Computational

We next examined the local dynamics of the polymer both as a function of hydration level of the silica surface as well as the distance from its surface using MD simulations. Among the various types of local motion found in polymer liquids, the change in the orientation of individual bonds with time is one that can be readily evaluated from the MD simulations. The bond reorientation motions are also amenable to experimental measurements such as NMR, though no explicit effort has been made to reproduce the NMR relaxation times due to the large number of calculations that would have to be performed for complete analysis of the numerous proton-proton pairs and the large range of time scales that influence the relaxation times [31]. Here we investigate the PDMS motional dynamics using the

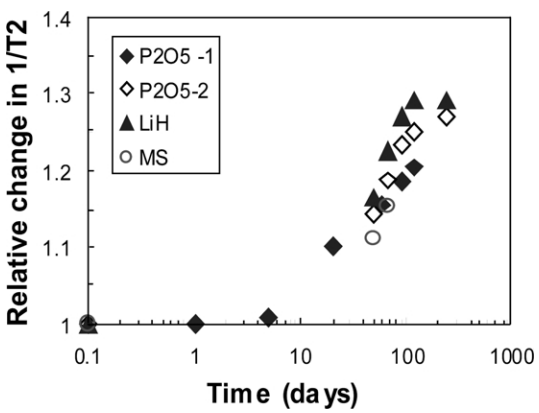

Fig. 2. Relative change in the inverse transverse relaxation time ($1/T_2$) as a function of time the filled PDMS/PDPS copolymer was stored under the desiccating agents indicated.

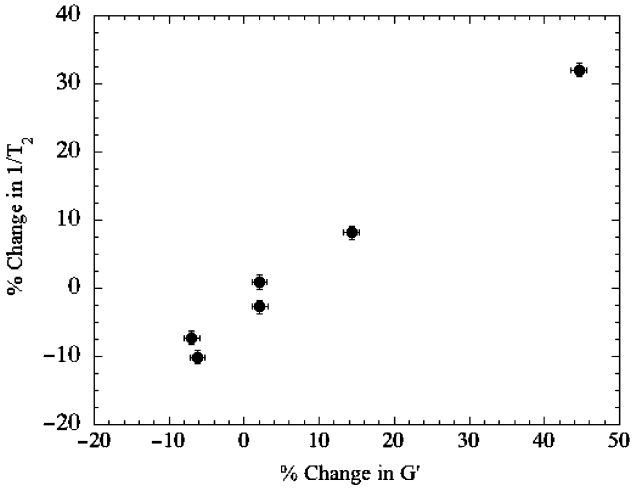

Fig. 3. Relative change in the inverse transverse relaxation time ($1/T_2$) as a function of the relative change in equilibrium storage modulus for various crosslink density copolymers. The crosslinks were modified by exposure to ionizing radiation.

following time autocorrelation function (ACF),

$$P_1(t) = \langle \mu(0) \cdot \mu(t) \rangle \tag{6}$$

where $\mu(t)$ is a unit vector and $\langle\ \rangle$ denotes an ensemble average over all such vectors. In particular, we have investigated the bond vector ACF between the silicon atom in the polymer backbone and the carbon atom of the pendent methyl groups ($Si-CH_3$). Fig. 4 shows $P_1(t)$ for PDMS at 550 K as a function of both hydration level of the silica surface for bond vectors near the silica surface (Fig. 4(a)) as well as a function of distance from the silica surface at a surface hydration level of $\sim$8 OH/100 Å^2 (Fig. 4(b)). It is readily apparent from Fig. 4(b) that the mobility of the polymer near the surface is diminished considerably as compared to those bond vectors found further from the surface. Comparison of the mobility of the polymer matrix at the silica surface to that of the bulk PDMS fluid show that the PDMS relaxation dynamics in the presents of the silica filler is slowed considerably at 550 K. The PDMS dynamics are also found to be affected by the hydration levels of the silica surface. The general trend is that the polymer mobility tends to decrease (increased relaxation times) as the hydration level decreases, thus effectively 'stiffening' the polymer matrix. This may be in part due to screening of the long-ranged electrostatic charge by the chemisorbed hydroxyl groups or physisorbed water in the interfacial region. To test this assumption, relaxation dynamics of non-charged analogues were studied. The results of these simulations show that the PDMS relaxation dynamics are slowed by roughly an order of magnitude at 550 K in the presence of the long-ranged electrostatic interactions.

The motional dynamics of PDMS, obtained from our simulations, as a function of hydration level of the silica filler exhibit the same functional trend as identified from NMR as presented in Fig. 3 (see Section 4.1 above), namely,

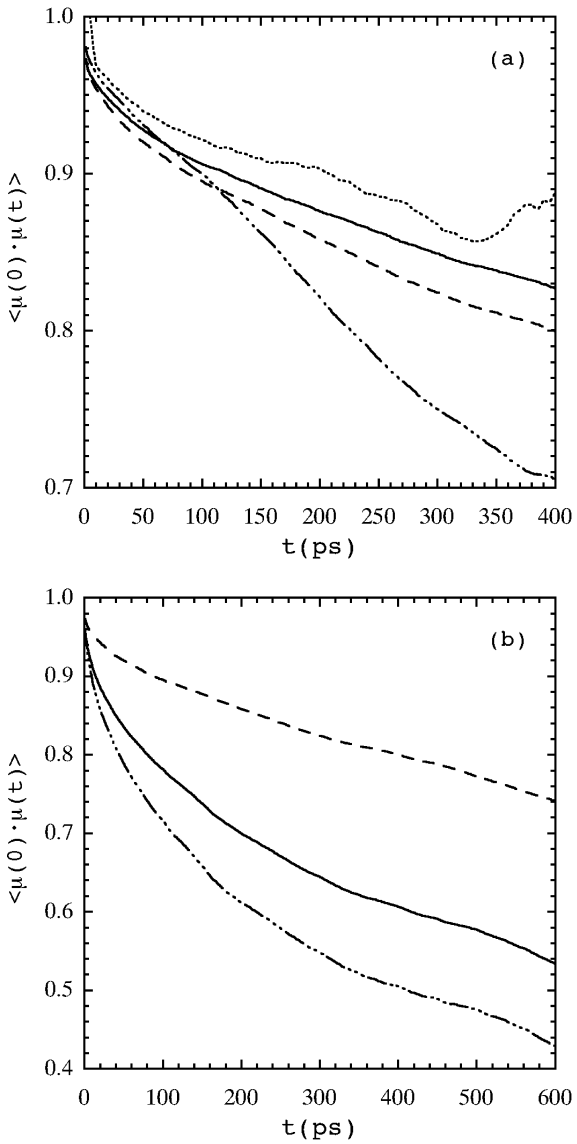

Fig. 4. The decay of $P_1(t)$ at 550 K. Panel a shows decay for those PDMS $Si-CH_3$ bond vectors closest to the silica surface as a function of surface hydration; dehydrated (dotted), ~4 OH/100 Å^2 (solid), ~8 OH/100 Å^2 (dashed), physisorbed water at surface (dash-dotted). Panel b shows bond vector decay as a function of contact distance from the silica surface at a hydration level of ~8 OH/100 Å^2; nearest to the surface (dashed), furthest from the surface (dash-dotted), all bond vectors (solid).

the relative 'stiffness' of the PDMS matrix is found to increase as the hydration level decreases.

To further understand the influence of the silica filler on the properties of the PDMS polymer, we investigate the structural properties of the silica filled PDMS composite by monitoring the local density distribution of the PDMS melt as a function of distance from the silica surface at 550 K. The local density is a convenient quantitative measure of the self-arrangement of the PDMS melt parallel to the filler surface. The effects of silica hydration dramatically affect the overall polymer structure. Tall and narrow peaks are observed in the immediate vicinity of the hydrated substrate (hydration level of ~8 OH/100 Å^2) that represent fluid layers and reflect the localized ordering of the polymer fluid at the silica surface (Fig. 5(a) and (c)). The local ordering lessens dramatically as the hydration level of the silica surface decreases such that the fluid layers become less distinct, and effectively absent at the dehydrated silica surface (Fig. 5(b) and (d)). The distance in which the order persists into the bulk fluid is also diminished as the hydration level decreases. Additionally, as the hydration level decreases, the contact distance between polymer and surface decrease by approximately 1.5 Å-the approximate size of a chemisorbed silanol groups. The overall decrease in structure of the PDMS polymer at the filler surface may in part describe the identifiable decrease in the heat of fusion, and the corresponding decrease in the melt temperature of the filled polymer systems as determined from DSC (see Section 4.1).

The role of the long-ranged Coulombic interactions in determining the structure and overall interactions between polymer and filler is also of interest. Studies such as this provide valuable insight into the 'tuneability' of the polymer material properties. To this end, simulations on the above systems have been performed with all the atomic charges set to zero. The resultant local density distributions are slightly different from their fully charged counterparts in that the detailed structure of the fluid layers as well as the magnitude of the local density was seen to diminish. The bifurcation seen in the first and second fluid layers due to the local structure of the oxygen moiety of the polymer backbone (Fig. 5(a)) is merged into a single peak in the *non*-Coulombic analogue, moreover, fewer distinct fluid layers are apparent in the *non*-Coulombic analogue (Fig. 5(c)). The overall distance of the PDMS fluid from the silica surface of the dehydrated and *non*-Coulombic analogue ensembles are reduced as compared to the hydrated and Coulombic ensembles (see Fig. 5). However, the closest contact between the silica surface and PDMS moieties is found to be between the silica surface hydrogen atoms (H) and PDMS oxygen backbone atoms (O), as identified by the intermolecular radial distribution, $g_{HO}(r)$ (Fig. 6). The structural difference seen between highly hydrated and dehydrated and Coulombic and *non*-Coulombic systems are consistent with the notion that the polymer–filler interactions are dominated by the long-ranged hydrogen bonding interactions and not solely based on the geometric constraints of packing the polymer close to the substrate surface. The carbon atoms of the PDMS methyl pendent groups and the PDMS backbone atoms are seen to be layered at the silica surface at the same relative distance from the substrate surface in the simulations unit cell. The more diffuse HH intermolecular radial distribution, $g_{HH}(r)$, peak is found to lie between the $g_{HC}(r)$ and $g_{HSi}(r)$ peaks (centered at ~3 Å) and the $g_{HO}(r)$ peak (centered at ~2 Å), as expected. The second PDMS fluid layer is centered at ~5.5 Å. No similar structural features are identified in the dehydrated and *non*-Coulombic analogue systems (see Supplementary Material).

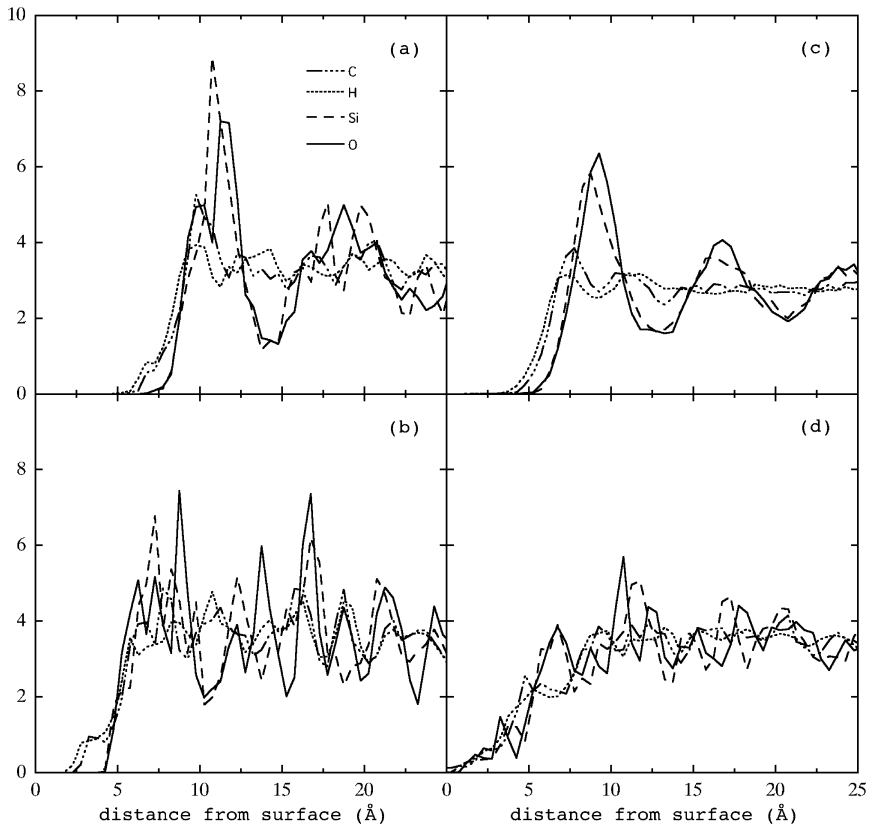

Fig. 5. Local density distribution of PDMS with Coulombic interactions (panels a and b) and without Coulombic interactions (panels c and d) at 550 K and a silica surface hydration level of ~8 OH/100 Å^2 (panels a and c) and dehydrated (panels b and d). Lines are labeled in panel a.

5. Conclusions

Our simulations reveal that the polymer–silica contact distance is decreased as the level of 'water' (both chemisorbed and physisorbed) in the interfacial region is decreased. In addition, 'water' in the interfacial region seems to screen the long-ranged interactions, mediating the polymer relaxation dynamics and ultimately increasing the polymer mobility. The 'water' in the interfacial region is also found to increase the overall PDMS structure as identified by both the local density distributions as well as the radial distribution functions, in particular the interaction between the oxygen backbone atoms of the PDMS fluid and the silanol surface groups (hydrogen bonding type interactions). We, therefore, suggest that the diminished local ordering, closer polymer-silica contact, and the loss of electrostatic 'screening' upon dehydration of the silica filler particles, as a possible mechanism for the reduced polymer mobility (overall polymer 'stiffening'). Further the decrease in both the heat of fusion and melt temperature is also attributed to the loss of 'water', as seen experimentally.

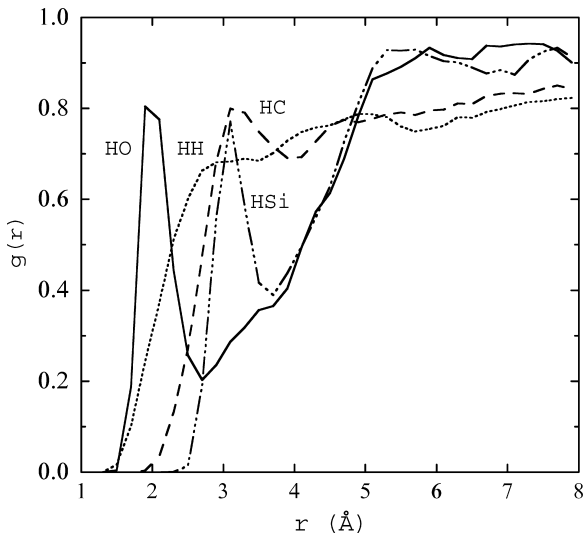

Fig. 6. Intermolecular radial distribution functions, $g_{ij}(r)$, versus the distance between the silica surface moieties (i = H, O, and Si) and PDMS polymer moieties (j = H, C, O, and Si) obtained from MD simulations at 550 K with Coulombic interactions hydration levels of either ~8 OH/100 Å^2. Lines are labeled in the figure.

Acknowledgements

We would like to thank both Rebecca Cohenour and Elizabeth Pravedel for performing the DSC studies and William Sung for performing the DMA studies. This work was performed under the auspices of the US Department of Energy by University of California Lawrence Livermore National Laboratory under contract No. W-7405-Eng-48.

References

[1] Kraus G. Rubber Chem Techol 1965;38:1070.
[2] Zeigher JM, Fearon FWG. Silicon based polymer science: a comprehensive resource. Washington, DC: ACS Press; 1990.
[3] Vondracek P, Pouchelon A. Rubber Chem Technol 1990;63:202.
[4] Ferry JD. Viscoelastic properties of polymers. New York: Wiley; 1980.
[5] Gee RH, Fried LE, Cook RC. Macromolecules 2001;34(9):3050.
[6] Hedenqvist MS, Bharadwaj R, Boyd RH. Macromolecules 1998;31: 1556.
[7] Meier RJ, Struik LCE. Polymer 1998;39:31.
[8] Han J, Boyd RH. Polymer 1996;37:1797.
[9] Gee RH, Boyd RH. Polymer 1995;36:1435.
[10] Gee RH, Boyd RH. J Chem Phys 1994;101:8028.
[11] Boyd RH, Gee RH, J H, Y J. J Chem Phys 1994;101:788.
[12] Han J, Gee RH, Boyd RH. Macromolecules 1994;27:7781.
[13] Boyd, RH. Atomistic modeling of physical properties of polymers, 1994. Berlin: Springer.
[14] Han J, Boyd RH. Macromolecules 1994;27:5365.
[15] Pant PVK, Han J, Smith GD, Boyd RH. J Chem Phys 1993;99:597.
[16] Sylvester MF, Yip S, Argon AS. Computer simulation of polymers. Englewood Cliffs, NJ: Prentice-Hall; 1991.
[17] Bordeaux D, Cohen-Addad JP. Polymer 1990;31(4):743–8.
[18] Molecular Simulations, Inc., San Diego, CA.
[19] Maple JR, Dinur U, Hagler AT. Proc Natl Acad Sci 1988;85:5350.
[20] Sun H. Polym Prepr 1992;33:657.
[21] Maple JA, Hwang M-J, Stockfisch TP, Dinur U, Waldman M, Ewig CS, Hagle AT. J Comp Chem 1994;15:162.
[22] Wilson EB, Decius JC, Cross PC. Molecular vibrations. New York: Dover; 1980.
[23] Ewald PP. Ann d Physik 1921;64:253.
[24] Karasawa N, Goddard WAI. J Phys Chem 1989;93:7320–7.
[25] Allen MP, Tildesley DJ:. Computer simulation of liquids. Oxford, UK: Clarendon Press; 1989.
[26] Andersen HC. J Chem Phys 1980;72:2384.
[27] Chien A, Maxwell RS, Chambers D, Balazs GB. Rad Phys Chem 2000;59:493.
[28] Maxwell RS, Balazs GB. J Chem Phys 2002;116:10492.
[29] Cohen-Addad JP. Progr NMR Spect 1993;25:1.
[30] Cohen-Addad JP, Domard M, Lorentz G, Herz J. J Phys (Les Ullis, Fr) 1984;45:575.
[31] Mehring M. High resolution NMR spectroscopy in solids. Berlin: Springer; 1983.
[32] Schneider M, Gasper L, Demco DE, Blümich B. J Chem Phys 1999; 111:402.
[33] Dollase T, Graf R, Heuer A, Spiess HW. Macromolecules 2001;34: 298.
[34] Graf R, Heuer A, Spiess HW. Phys Rev Lett 1998;80:5738.
[35] Graf R, Demco DE, Hafner S, Spiess HW. Solid State NMR 1998;12: 139.
[36] Gronski W, Hoffmann U, Simon G, Wutzler A, Straube E. Rubber Chem Techol 1992;65:63.
[37] Maxwell RS, Balazs B. Nucl Instrum Methods Phys Res B 2003;208: 199–203.